Volume 12, Number 2, 2019. pp. 133-140

Jordan Journal of Physics

ARTICLE

Structural, Spectroscopic and Magnetic Characterization of $Bi_{0.9}X_{0.1}Fe_{0.98}Mg_{0.02}O_3$ (X = Gd, Sm, Ba) Multiferroic Compounds

Mansour M. Al-Haj

Physics Department, Mutah University, Mutah, Al-Karak, Jordan.

Received on: 08/06/2018; Accepted on: 8/10/2018

Abstract: The compounds $Bi_{0.9}Gd_{0.1}Fe_{0.98}Mg_{0.02}O_3$, $Bi_{0.9}Sm_{0.1}Fe_{0.98}Mg_{0.02}O_3$ and $Bi_{0.9}Ba_{0.1}Fe_{0.98}Mg_{0.02}O_3$ were found to have a rhombohedral perovskite-like structure. The structural parameters were extracted from the X-ray diffraction data. Fourier transform infrared spectroscopy revealed traces of the α-Fe_2O_3 magnetic phase in the $Bi_{0.9}Ba_{0.1}Fe_{0.98}Mg_{0.02}O_3$ compound. The $Bi_{0.9}Gd_{0.1}Fe_{0.98}Mg_{0.02}O_3$ and $Bi_{0.9}Sm_{0.1}Fe_{0.98}Mg_{0.02}O_3$ compounds were found to show a weak intrinsic ferromagnetic behavior, whereas the ferromagnetism of the $Bi_{0.9}Ba_{0.1}Fe_{0.98}Mg_{0.02}O_3$ compound was found to be non-intrinsic in origin. The magnetic transition temperatures were found to be around 340 °C.

Keywords: X-ray diffraction, Spectroscopy, Magnetization, Transition temperature.
PACS: 61.05.cp; 75.50.Ee; 75.60.Ej.

1. Introduction

Multiferroics are materials that exhibit more than one ferro-property (ferromagnetism, ferroelectricity, ferroelasticity) simultaneously in the same phase. Multiferroics include also non-primary order parameters, such as antiferromagnetism or ferrimagnetism. The inorganic compound $BiFeO_3$ (BFO) with perovskite-like structure is one of the most fascinating multiferroic materials [1]. The room-temperature phase of BFO is classified as rhombohedral with space group R3c. It is synthesized in bulk [2], nanoparticles [3-5], single crystal [6], thin film [7], nanotubes [8] or nanowires [9] form. Its antiferromagnetic (G-type magnetic ordering) Neel temperature $T_N \cong$ 370 °C and its ferroelectric Curie temperature T_C $\cong$ 827 °C. Ferroelectric polarization occurs along the pseudocubic direction $\langle 111 \rangle_c$ with a magnitude of 90-100 $\mu C/cm^2$, depending on the material's form. However, the bulk form is suffering from shortcomings, such as weak magnetization and high leakage current, which prohibit its applicability in future electronic devices. Therefore, there has been an extensive research work in order to improve the performance of this material. Partial substitution of Bi^{3+} by ions such as Y^{3+} [10, 11], Dy^{3+} [12], Gd^{3+} [13, 14], Ho^{3+} [15], Nd^{3+} [16], Tb^{3+} [17], Sr^{2+} [18]; partial substitution of Fe^{3+} by ions such as Mn^{3+} and Co^{3+} [19]; or partial co-substitution of Bi^{3+} and Fe^{3+} by ions such as (Sm^{3+}, Sc^{3+}) [20], (Ba^{2+}, Mn^{3+}) [21], (In^{3+}, Mn^{3+}) [22], (Gd^{3+}, Ti^{4+}) [23], (Ca^{2+}, Ti^{4+}) [24], (La^{3+}, Ti^{4+}) [25], (K^+, Ta^{5+}) [26], (Eu^{3+}, Mn^{2+}) [27], (La^{3+}, V^{5+}) [28], all these substitutions were found to enhance the structural, electric, magnetic, dielectric, optical, and ferroelectric properties of BFO and helped understand the behavior of this material. Despite the progress achieved, the story is not ending. There are still unanswered questions about the true origin of magnetism in BFO-substituted materials.

In this work, we investigate the multiferroic compounds $Bi_{0.9}Gd_{0.1}Fe_{0.98}Mg_{0.02}O_3$, $Bi_{0.9}Sm_{0.1}Fe_{0.98}Mg_{0.02}O_3$ and $Bi_{0.9}Ba_{0.1}Fe_{0.98}Mg_{0.02}O_3$ by several techniques.

Corresponding Author: Mansour M. Al-Haj **Email**: mansour@mutah.edu.jo

Throughout this paper, we refer to them as GdMg, SmMg and BaMg, respectively. Since the ionic radius $r(\mathrm{Mg}^{2+}) = 0.720$ Å > $r(\mathrm{Fe}^{3+}) = 0.645$ Å, only 2% of Fe^{3+} ions were replaced by Mg^{2+} ions to make sure that they go into the Fe^{3+} sites and stabilize the crystal structure.

2. Experimental Methods

The compounds were prepared by the conventional mixed oxide method. Stoichiometric amounts of pure oxides of Bi_2O_3, Gd_2O_3, Sm_2O_3, Fe_2O_3 and MgO were mixed and ground in an agate mortar and pestle for half an hour. The GdMg and SmMg mixtures were calcined at 825 °C in a tube furnace for 90 min. After the calcination process, the two mixtures were cooled to room temperature, ground and calcined again at 825 °C for 90 min. Then, the mixtures were cooled to room temperature and ground to get a fine powder. The same procedure was done to the BaMg mixture, but with the first calcination at 825 °C for 60 min and the second one at 825 °C for 75 min. The x-ray diffraction (XRD) patterns were collected by a Seifert 3003TT powder diffractometer using CuK_α radiation. The Fourier transform infrared (FTIR) spectra of the samples were collected by a JASCO E300 spectrometer (range: 400 - 4000 cm^{-1}). Since potassium bromide (KBr) does not show any absorption spectrum in the IR region, a small amount of each powder (1% by weight) is mixed by KBr (99% by weight) and then pressed into thin pellets (thickness < 1 mm) for FTIR spectra collection. The magnetic hysteresis loops were recorded by a conventional vibrating sample magnetometer (VSM) calibrated with a nickel sphere. The magnetic transition temperature was measured by a Mettler differential scanning calorimeter (DSC) with a maximum operating temperature of 450 °C. The instrument was calibrated with an indium standard and aluminum sample holders were used for measurement.

3. Results and Discussion

Fig. 1 shows the XRD patterns of the GdMg, SmMg, and BaMg compounds. The reflection peaks in these patterns were indexed according to the $BiFeO_3$ diffraction pattern (PDF # 86-1518), confirming the rhombohedral perovskite-like structure with space group R3c. However, small traces of the impurity nonmagnetic phases mullite $Bi_2Fe_4O_9$ (indicated by •) and sillenite $Bi_{25}FeO_{40}$ (indicated by ♦) are existent. These are the inevitable impurity phases that were reported to form during the synthesis of related BFO-substituted compounds [29] and are attributed to the volatilization of Bi.

In order to extract accurate values of the structural parameters of the studied materials, we carried out a least-squares refinement calculation of the XRD data using the UnitCell program [30]. The lattice parameters a and c, as well as the volume V of the hexagonal unit cell are listed in Table 1. Since $r(\mathrm{Ba}^{2+}) = 1.35$ Å > $r(\mathrm{Sm}^{3+}) = 0.958$ Å > $r(\mathrm{Gd}^{3+}) = 0.938$ Å, the general trend is that the structural parameters increase as the radius of the substituting ion is increased (the c value of BaMg has undergone a slight decrease, but the a and V values have increased).

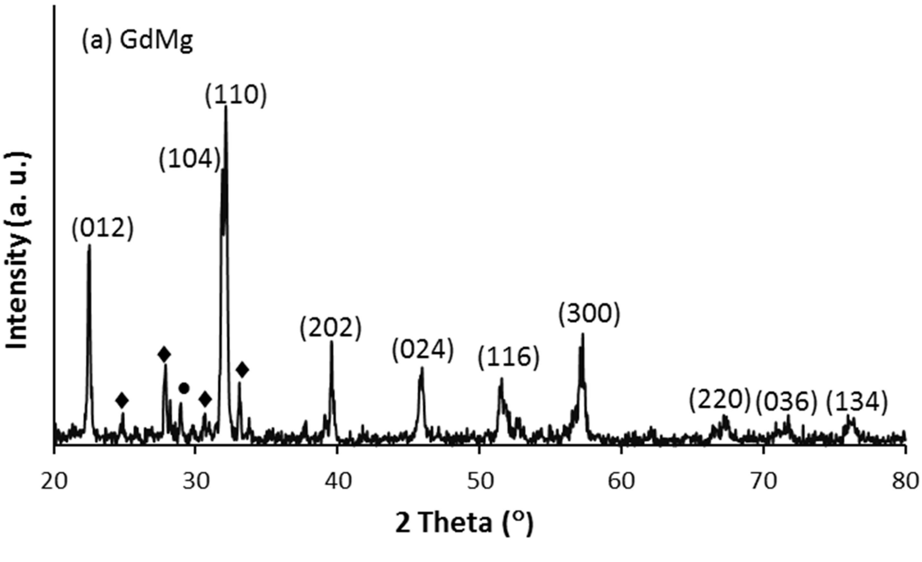

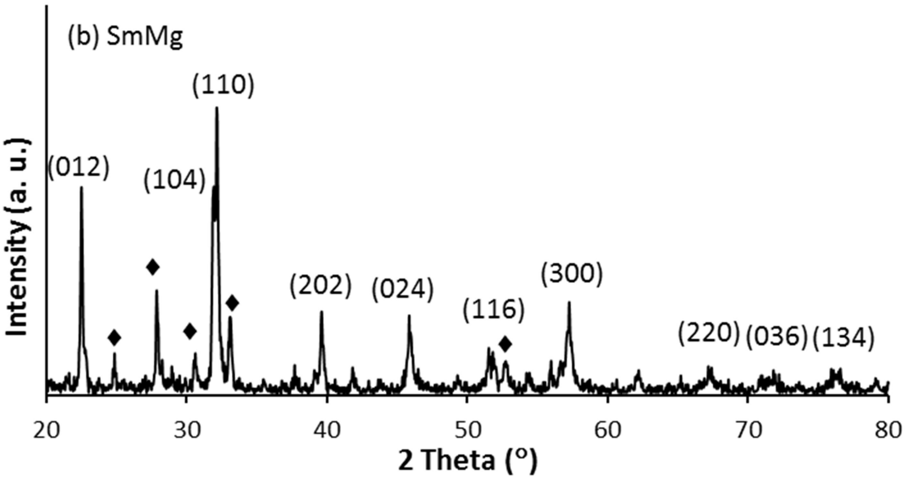

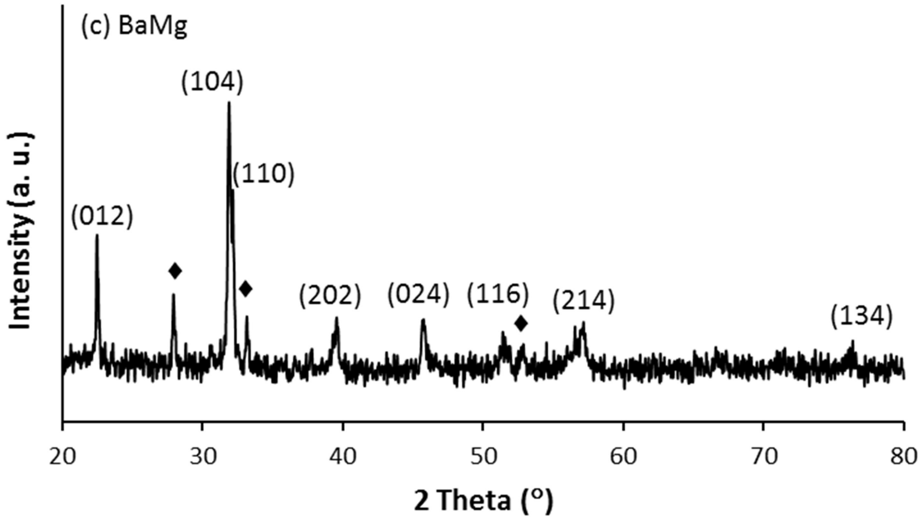

FIG. 1. The XRD patterns of (a) GdMg, (b) SmMg and (c) BaMg.

TABLE 1. The structural parameters of the studied compounds.

Compound	*a* (Å)	*c* (Å)	*V* (Å^3)
GdMg	5.5685 ± 0.0003	13.7794 ± 0.0018	370.04 ± 0.05
SmMg	5.5691 ± 0.0003	13.7900 ± 0.0018	370.39 ± 0.05
BaMg	5.5767 ± 0.0005	13.7863 ± 0.0020	371.31 ± 0.05

It should be observed from the table that, due to the small difference between the radii of Gd^{3+} and Sm^{3+}, the cell volume has undergone a small change, but this is not the case for Ba^{2+} which has a relatively large radius. In conclusion, the substituting process has caused a lattice distortion (greatest for BaMg) which manifests itself in a change in the Bi/Fe-O bond length and the Fe-O-Fe bond angle [15, 27].

Another important point that we want to consider is the existence of traces of the magnetic phases Fe_3O_4 (PDF # 87-2334), $BaFe_2O_4$ (PDF # 70-1441) and/or α-Fe_2O_3 (PDF # 33-0664). In fact, a careful search-match process did not reveal any traces of the ferrite phases Fe_3O_4 and $BaFe_2O_4$ in all compounds. Moreover, it was hard to discover traces of the hematite phase α-Fe_2O_3 using the search-match process due to the proximity of the strong (104) reflection peak of α-Fe_2O_3 to the (321) reflection peak of $Bi_{25}FeO_{40}$ (PDF # 78-1543). But, as we will see, traces of the hematite phase do exist in the BaMg compound.

FTIR spectroscopy is an analytical technique used to measure the absorption of infrared radiation by the sample material *versus* wavelength. The infrared absorption bands identify the vibrational modes of the building units. Fig. 2 shows the FTIR spectra for the GdMg, SmMg and BaMg compounds in the wavenumber range 400 - 2000 cm^{-1}. The absorption peaks at 573, 575 and 567 cm^{-1}

(indicated by vertical lines) correspond to the Fe-O stretching vibrations in the FeO_6 octahedral unit of each compound. In the FTIR spectra of GdMg and SmMg, we can see two prominent peaks at 455 and 457 cm^{-1} (indicated by x's), corresponding to the O-Fe-O bending vibrations. Four additional non-intrinsic prominent absorption peaks (at 824, 877, 1036 and 1449 cm^{-1}) can be observed in the BaMg spectrum.

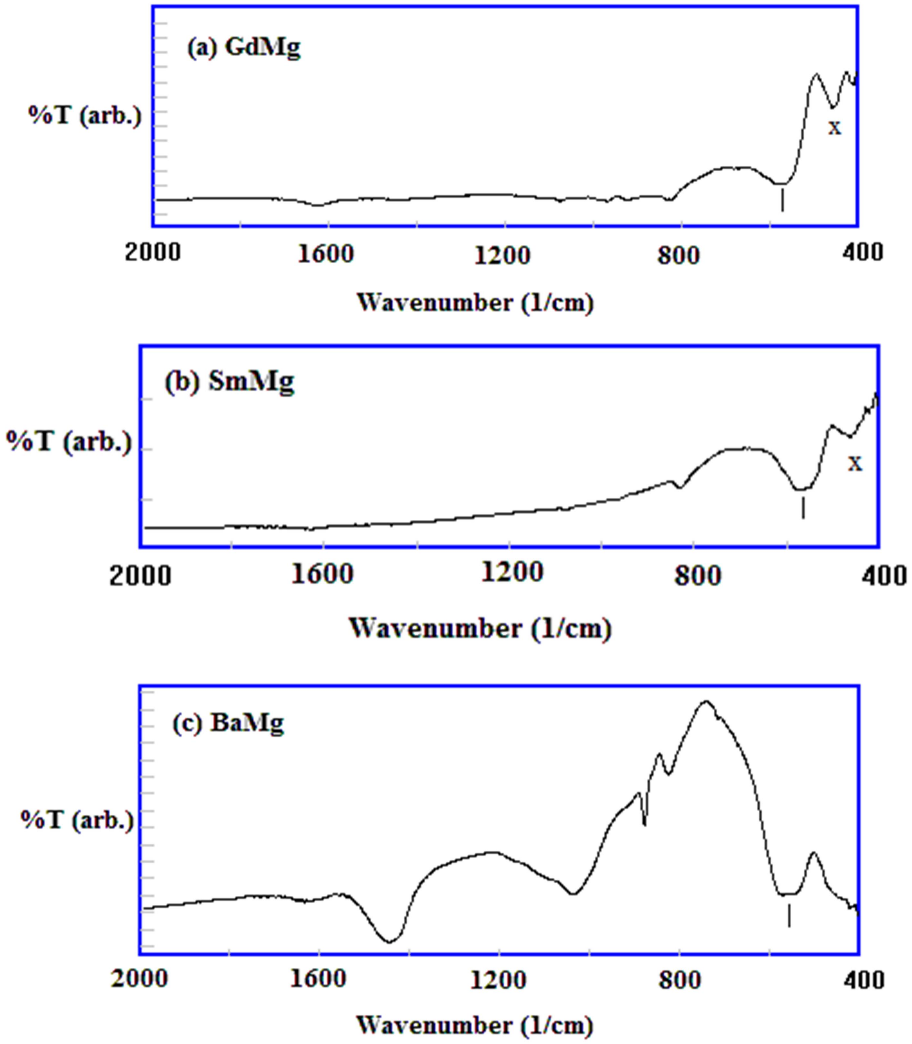

FIG. 2. The FTIR spectra of (a) GdMg, (b) SmMg and (c) BaMg.

Some researchers reported two peaks at 815 and 878 cm^{-1} (close to our first two values) in the FTIR spectrum of Ho-substituted BFO [15] that were attributed to the absorption of water and CO_2 from the environment. In fact, we checked up the FTIR spectra of water and CO_2 in the NIST WebBook and found that these peaks cannot be attributed to water and CO_2; they are better attributed to the α-Fe_2O_3 hematite phase (the NIST WebBook). The last two peaks in the BaMg spectrum could have resulted from other unidentified impurities (probably in KBr).

The room temperature hysteresis loops of the compounds are shown in Fig. 3. It is seen that the compounds GdMg and SmMg exhibit weak ferromagnetism with unsaturated magnetization. The BaMg compound exhibits an enhanced ferromagnetic behavior with an open hysteresis loop. Since the concentration of Mg^{2+} ions in all compounds is the same, the effect of these ions on the magnetization is invariant. The values of the remnant magnetization M_r and coercive field H_c are listed in Table 2. It is known that there are several reasons for the appearance of weak ferromagnetism in BFO-substituted compounds. They include suppression of the helical spin structure of BFO due to lattice distortion, change of the oxidation state of the substituting ions, creation of oxygen vacancies, magnetic impurities and/or chemical inhomogeneity. As seen in Table 2, the M_r value of SmMg is 0.0388 emu/g and that of GdMg is 0.0924 emu/g, which is about 2.4 greater than that of SmMg. Such a difference cannot be explained solely based on lattice distortion and/or oxygen vacancies, since, as we mentioned earlier, the lattice distortion in each compound is nearly the same as there is no much difference between the ionic radii of Gd^{3+} and Sm^{3+} and both ions have the same oxidation state so the that effect of oxygen vacancies is nullified. We think that the plausible explanation is that, since the magnetic moment of Gd^{3+} is greater than that of Sm^{3+}, both ions doped at the Bi^{3+} sites would cause magnetic coupling interactions with the Fe^{3+} ions (the Gd^{3+}-Fe^{3+} interaction is greater and would lead to enhancement of ferromagnetism in the GdMg compound).

Now let's get back to BaMg, which has an M_r value of 0.857 emu/g (greater than the GdMg value by a factor of about 9.3). Ba^{2+} ions doped at the Bi^{3+} sites are not magnetic and as we have seen, lattice distortion is the greatest in BaMg. But, this is not sufficient to cause such a large change in ferromagnetism. We think that the real cause of such a relatively large magnetization is the parasitic α-Fe_2O_3 hematite phase, which is a soft ferromagnet at room temperature and masks the intrinsic magnetization of the sample. This result is in agreement with other reported investigations [31, 32]. But, what is the reason for the large value of H_c? In fact, the role of oxygen vacancies cannot be overlooked. Since the oxidation state of Ba^{2+} is different from that of Bi^{3+}, charge neutrality in BaMg is accomplished *via* the creation of oxygen vacancies: structural defects that increase magnetic anisotropy and, consequently, increase the value of H_c.

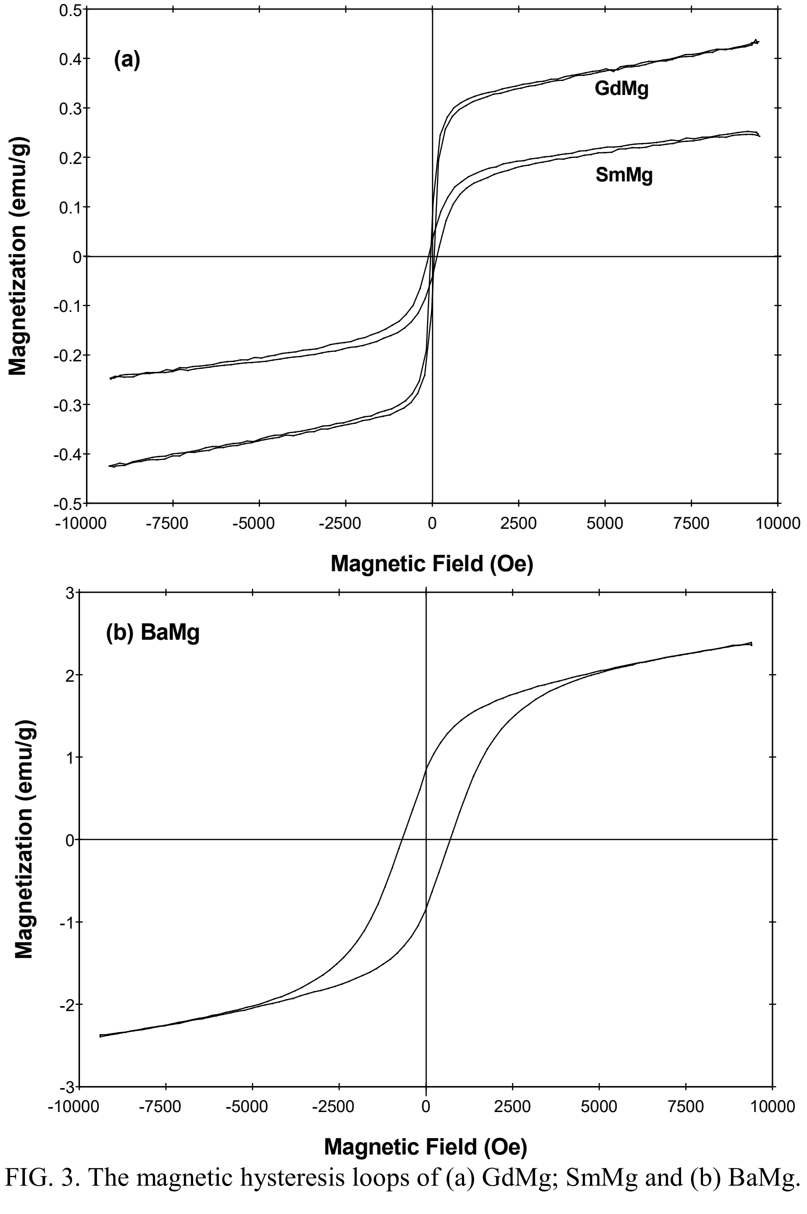

FIG. 3. The magnetic hysteresis loops of (a) GdMg; SmMg and (b) BaMg.

TABLE 2. Some magnetic parameters of the compounds.

Compound	M_r (emu/g)	H_c (Oe)	T_N (°C)
GdMg	0.0924	70	343
SmMg	0.0388	107	341
BaMg	0.857	693	340

DSC is a thermal technique that can be used to measure a number of characteristic properties of a sample, such as fusion, crystallization, oxidation and glass transition. One less common use of DSC is to identify the magnetic transition temperature T_N, which is revealed by a weak endothermic peak on the DSC scan. In practice, such a peak is hard to detect, because it could overlap with other noisy signals, especially if the baseline is fluctuating with temperature. Nonetheless, by the proper choice of sample mass and heating rate, the transition can be detected. Fig. 4 shows the DSC scans of the compounds and their magnetic transition temperatures are listed in Table 2. Taking into consideration that $T_N \cong 370$ °C for pure BFO, the obtained values seem to be reasonable. Comparatively, a magnetic transition temperature of 350 °C was reported for $Bi_{0.95}Sr_{0.05}FeO_3$ using DSC [18]. Based on the weak magnetism of these materials, the T_N values obtained are nearly the same.

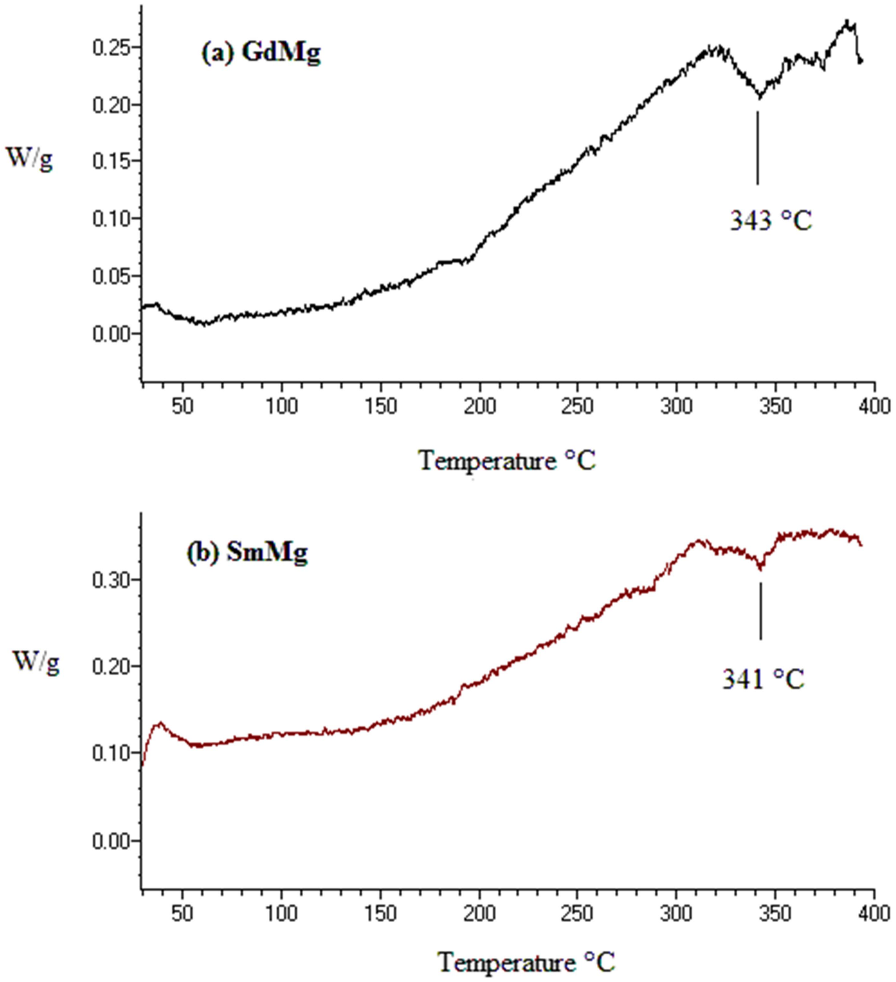

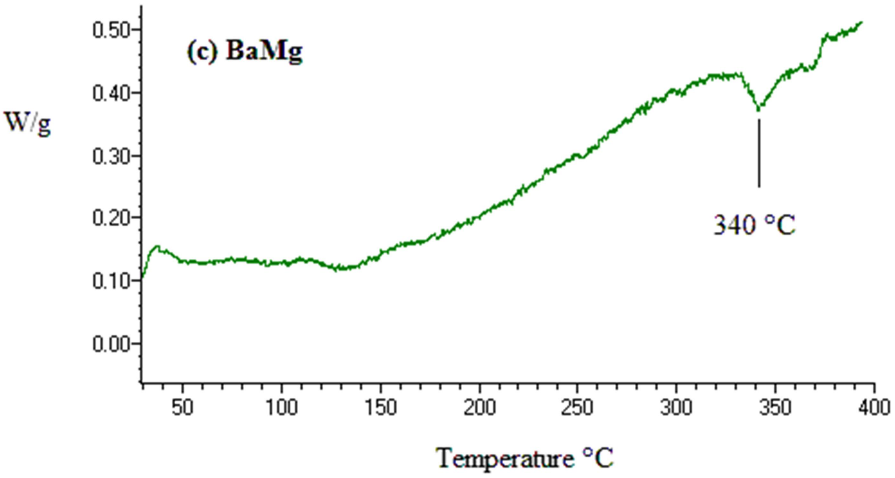

FIG. 4. The DSC curves of (a) GdMg, (b) SmMg and (c) BaMg.

4. Conclusions

We have carried out a comparative study of the structural and magnetic properties of the compounds GdMg, SmMg and BaMg, prepared by the mixed oxide method. They have been explored by structural, spectroscopic, magnetic and thermal techniques. We have found that the magnetization of GdMg and SmGd is intrinsic in origin, while that of BaMg is masked by the impurity magnetic phase. One has to be very careful in explaining the magnetic data, because otherwise misleading results would be obtained.

References

[1] Catalan, G. and Scott, J.F., Adv. Mater., 21 (2009) 2463.

[2] Singh, H. and Yadav, K.L., Ceramics Inter., 41 (2015) 9285.

[3] Wei, J. and Xue, D., Mater. Res. Bull., 43 (2008) 3368.

[4] Alemi, A. and Purhasan, A., J. Mater. Sci.: Mater. Electron., 28 (2017) 14476.

[5] Maleki, H., Haselpour, M. and Fathi, R., J. Mater. Sci.: Mater. Electron., 29 (2018) 4320.

[6] Haumont, R., Saint-Martin, R. and Byl, C., Phase Trans., 81 (2008) 881.

[7] Ali, Z., Atta, A., Abbas, Y., Sedeek, K., Adam, A. and Abdeltwab, E., Thin Solid Films, 577 (2015) 124.

[8] Wu, L., Sui, W., Dong, C., Zhang, C. and Jiang, C., Appl. Surf. Sci., 384 (2016) 368.

[9] Lotey, G.S. and Verma, N.K., Mater. Sci. Semicond. Process., 21 (2014) 206.

[10] Gómez, J., Canaria, C., Burgos, R., Ortiz, C., Supelano, G. and Vargas, C., J. Phys.: Conf. Ser., 687 (2016) 012091.

[11] Wu, Y.J., Qin, Z.X., Chen, X.K., Zhang, J., Liu, J., Wu, Z. and Chen, X.J., J. Phys.: Condens. Matter, 25 (2013) 365401.

[12] Uniyal, P. and Yadav, K.L., J. Phys.: Condens. Matter, 21 (2009) 012205.

[13] Kumar, S., J. Mater. Sci.: Mater. Electron., 24 (2013) 2112.

[14] Sharma, S., Mishra, A., Saravanan, P., Pandey, O.P. and Sharma, P., J. Magn. Magn. Mater., 418 (2016) 188.

[15] Singh, H. and Yadav, K.L., J. Phys. D: Appl. Phys., 48 (2015) 205001.

[16] Zhang, H., Liu, W.F., Wu, P., Hai, X., Wang, S.Y., Liu, G.Y. and Rao, G.H., J. Nanopart. Res., 16 (2014) 2205.

[17] Guo, M.C., Liu, W.F., Wu, P., Zhang, H., Xu, X.L., Wang, S.Y. and Rao, G.H., Chin. Phys. Lett., 32 (2015) 066101.

[18] Mandal, S., Rakshit, T., Ray, S., Mishra, S., Krishna, P. and Chandra, A., J. Phys.: Condens. Matter, 25 (2013) 055303.

[19] Ma, Y., Tang, X., Lu, M., Zheng, K., Mao, W., Zhang, J., Yang, J. and Li, X., J. Supercond. Nov. Magn., 28 (2015) 3593.

[20] Wang, C.A., Pang, H.Z., Zhang, A.H., Qin, M.H., Lu, X.B., Gao, X.S., Zeng, M. and Liu, J.M., J. Phys. D: Appl. Phys., 48 (2015) 395302.

[21] Kumar, K.S., Venkateswaran, C., Kannan, D., Tiwari, B. and Rao, M.S.R., J. Phys. D: Appl. Phys., 45 (2012) 415302.

[22] Arya, G.S. and Negi, N.S., J. Phys. D: Appl. Phys., 46 (2013) 095004.

[23] Ahmmad, B., Islam, M., Billah, A. and Basith, M., J. Phys. D: Appl. Phys., 49 (2016) 095001.

[24] Khomchenko, V. and Paixão, J., J. Phys.: Condens. Matter, 27 (2015) 436002.

[25] Kumar, P., Panda, C. and Kar, M., Smart Mater. Struct., 24 (2015) 045028.

[26] Mohanty, S., Kumar, A. and Choudhary, R.N.P., J. Mater. Sci.: Mater. Electron., 26 (2015) 9640.

[27] Zhu, Y., Quan, C., Ma, Y., Wang, Q., Mao, W., Wang, X., Zhang, J., Min, Y., Yang, J., Li, X. and Huang, W., Mater. Sci. Semicond. Process., 57 (2017) 178.

[28] Yu, B., Li, M., Wang, J., Pei, L., Guo, D. and Zhao, X., J. Phys. D: Appl. Phys., 41 (2008) 185401.

[29] Al-Haj, M., Turk. J. Phys., 36 (2012) 415.

[30] Holland, T. and Redfern, S., Mineral. Mag., 61 (1997) 65.

[31] Al-Haj, M., Cryst. Res. Technol., 45 (2010) 1145.

[32] Nayek, C., Tamilselvan, A., Thirmal, C., Murugavel, P. and Balakumar, S., J. Appl. Phys., 115 (2014) 073902.